JACS
JOURNAL OF THE AMERICAN CHEMICAL SOCIETY
pubs.acs.org/JACS
Communication

Unimolecular Polypeptide Micelles via Ultrafast Polymerization of *N*-Carboxyanhydrides

Shixian Lv, Hojun Kim, Ziyuan Song, Lin Feng, Yingfeng Yang, Ryan Baumgartner, Kuan-Ying Tseng, Shen J. Dillon, Cecilia Leal, Lichen Yin,* and Jianjun Cheng*

Cite This: *J. Am. Chem. Soc.* 2020, 142, 8570−8574

ABSTRACT: Polypeptide micelles are widely used as biocompatible nanoplatforms but often suffer from their poor structural stability. Unimolecular polypeptide micelles can effectively address the structure instability issue, but their synthesis with uniform structure and well-controlled and desired sizes remains challenging. Herein we report the convenient preparation of spherical unimolecular micelles through dendritic polyamine-initiated ultrafast ring-opening polymerization of *N*-carboxyanhydrides (NCAs). Synthetic polypeptides with exceptionally high molecular weights (up to 85 MDa) and low dispersity ($Đ$ < 1.05) can be readily obtained, which are the biggest synthetic polypeptides ever reported. The degree of polymerization was controlled in a vast range (25−3200), giving access to nearly monodisperse unimolecular micelles with predictable sizes. Many NCA monomers can be polymerized using this ultrafast polymerization method, which enables the incorporation of various structural and functional moieties into the unimolecular micelles. Because of the simplicity of the synthesis and superior control over the structure, the unimolecular polypeptide micelles may find applications in nanomedicine, supermolecular chemistry, and bionanotechnology.

Polymeric micelles have attracted enormous attention for applications in drug/gene delivery.[1,2] Conventional polymeric micelles are spherical and prepared by self-assembly of amphiphilic copolymers, which is driven by various intermolecular forces such as hydrophobic and electrostatic interactions.[3−6] However, several key drawbacks of polymeric micelles have limited their potential as delivery vehicles for clinical applications. Polymeric micelles are usually heterogeneous mixtures consisting of not only micelles but also free polymers, even above the critical micelle concentration (CMC),[7,8] making them very challenging for chemistry, manufacturing, and controls in micellar drug development. Despite the ease of preparation via copolymer self-assembly, polymeric micelles generally suffer from their structural instability[9,10] and may easily disassemble to free polymers under dilute conditions or when exposed to environmental variations (e.g., pH and ionic strength).[11,12] These drawbacks have hindered the applications of polymeric micelles. Clinical success has been limited to only a few specific systems, although micellar drug delivery systems have been studied for two or three decades.

To overcome the instability of self-assembled micelles, efforts have been made to develop cross-linking strategies or design unimolecular micelles.[13−16] Unimolecular micelles are defined as a type of macromolecules having a three-dimensional/colloidal structure analogous to conventional micelles but with the polymer chains covalently bound together.[17−19] Because of this unique architecture, unimolecular micelles possess excellent stability against extreme conditions.[20−23] Unimolecular micelles, including dendrimers, hyperbranched polymers, and cylindrical brushes, are usually prepared via step-by-step synthesis or polymerization.[24−28] However, these methods still have limitations. For instance, step-by-step synthesis is able to produce monodisperse polymers but is only economical for low molecular weights (MWs). Polymerization methods (e.g., grafting-through/from) can give high MWs, but the control of polymers at high MWs (e.g., >10^6 Da) is still unsatisfactory for most polymerization systems.[29−31] Therefore, the development of simple methods to prepare unimolecular micelles with predictable size and low dispersity is still in high demand.

Recently, a polypeptide-based cooperative polymerization in solvents with low dielectric constants such as dichloromethane (DCM) was reported.[32,33] The unique feature in this polymerization is that the polymer's chain growth is catalyzed by its own macromolecular structure. The system consists of a linear scaffold with a high density of initiating groups from which amino acid *N*-carboxyanhydride (NCA) monomers can grow into polypeptide brushes. After reaching a critical chain length, the polypeptides fold into α-helices, which dramatically enhance the polymerization rate through their cooperative macrodipole interactions among neighboring α-helices.[32] We hypothesized that a cooperative NCA polymerization similar to that observed with a brush macroinitiator may proceed on the spherical surface of macroinitiators in proximity (Scheme 1), allowing synthesis of uniform polypeptide unimolecular micelles with the same spherical morphology adopted by most polymeric micelles.

Received: January 30, 2020
Published: March 20, 2020

https://dx.doi.org/10.1021/jacs.0c01173
J. Am. Chem. Soc. 2020, 142, 8570−8574

Scheme 1. Spherical Unimolecular Micelles from Surface NCA Polymerization

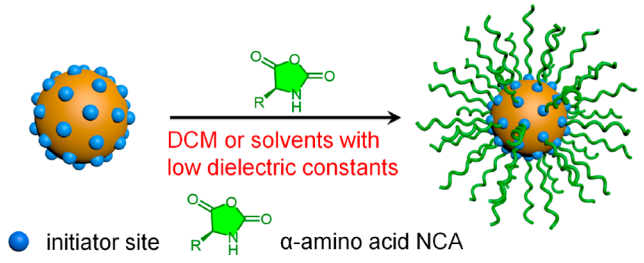

To validate this hypothesis, we selected polyamidoamine (PAMAM) dendrimers as the macroinitiators (denoted as G*x*, where *x* is the generation) because they adopt a nearly spherical structure and the primary amines anchored on the surface can serve to initiate NCA polymerization. γ-Benzyl-$_L$-glutamate NCA (BLG-NCA) was chosen as a model monomer because of its convenient synthetic and purification processes and good solubility in various solvents. The resulting polymer, poly(γ-benzyl-$_L$-glutamate) (PBLG), is known to adopt an α-helical conformation under various conditions,[34,35] thus allowing acceleration of the polymerization through interhelix cooperative macrodipole interactions. The polymerization was first performed in DCM with a low dielectric constant, which minimized the disruption of the macrodipole interactions between α-helices. The obtained polymers with different degrees of polymerization (DPs) are denoted as G*x*-*g*-PBLG$_n$ (where *n* is the designed DP), and gel permeation chromatography (GPC) was utilized to characterize the MWs of the polymers. The DP values refer particularly to the feeding ratio of the monomer to the primary amines of PAMAM.

In DCM, the polymerization of BLG-NCA conducted with different PAMAM macroinitiators resulted in polypeptides with predictable MWs and low dispersities (Figure 1b and Table S1). GPC light scattering (LS) and differential refractive index (dRI) responses demonstrated the monomodal distributions for all of the resulting polymers (Figures S1 and S2).

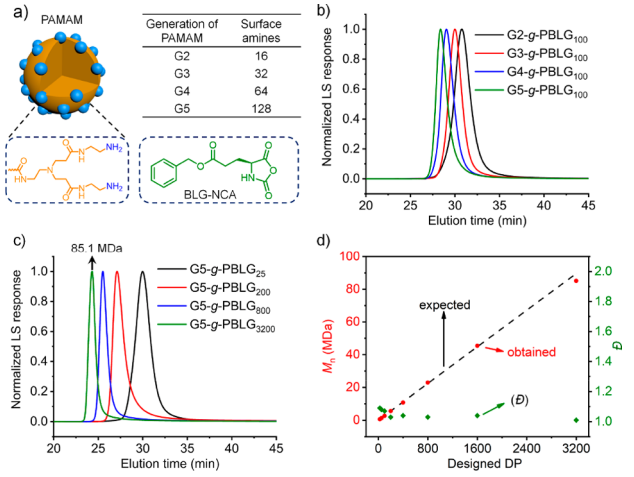

Figure 1. (a) Chemical structures of PAMAM and BLG-NCA. (b) GPC traces of polymers synthesized from different PAMAM initiators. (C) GPC traces of polymers synthesized from G5 at various designed DPs. (D) MWs and dispersities of G5-*g*-PBLG polymerized in DCM at $[M]_0/[I]_0$ ratios from 25 to 3200.

In addition, such controlled polymerization can proceed at monomer/initiator ratios ($[M]_0/[I]_0$, where the initiator refers to total primary amines) ranging from 25 to 3200, yielding polymers with predictable MWs (Figures 1c and S3 and Table S2). The dispersity values remained low at the extremely high DP of 3200 ($Đ$ < 1.05; Figure 1d). Further addition of monomers into the pre-existing polymer can successfully extend the polymer chains with low dispersity and expected MW, indicating the living feature of the polymerization (Figure S4). Moreover, the polymerization featured almost complete monomer conversions (>98%) even at extremely high DPs, yielding polymers of exceptionally high MW via a one-pot reaction (Table S2). The G5-inititated polymerization at the $[M]_0/[I]_0$ ratio of 3200 yielded the synthetic polypeptide with highest DP and MW ever reported (M_n = 8.5 × 10^7 Da), almost 20-fold bigger than the largest protein identified previously (titin, ∼4000 kDa).[36]

Such elegant control of the polymerization in DCM indicated that the PAMAM-initiated NCA polymerization may also follow a cooperative manner due to the proximity of α-helices. To verify this assumption, *in situ* Fourier transform infrared (FT-IR) spectroscopy was utilized to monitor the detailed progress of the polymerization (Figure 2a). It was

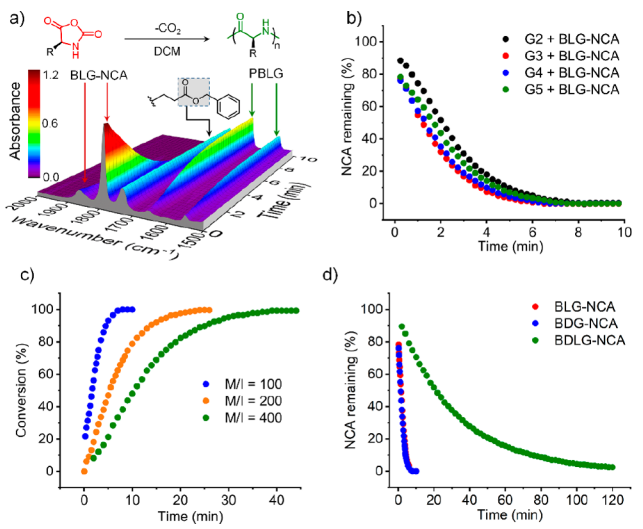

Figure 2. (a) FT-IR spectra showing the conversion of BLG-NCA initiated by G5 in DCM. (b) Conversion of BLG-NCA initiated by different PAMAM initiators at the $[M]_0/[I]_0$ ratio of 100. (c) Conversion of BLG-NCA initiated by G5 at various $[M]_0/[I]_0$ ratios. (d) Conversion of BLG-NCA, BDG-NCA, and BDLG-NCA initiated by G5 at the $[M]_0/[I]_0$ ratio of 100. All of the polymerizations were conducted in DCM.

noted that the surface NCA polymerization occurred at a very high rate in DCM, similar to the previously published brush polymerization system.[32] In particular, at the $[M]_0/[I]_0$ ratio of 100, NCA conversion was >99% within 8 min (Figure 2b), and at the higher $[M]_0/[I]_0$ ratio of 400, the polymerization was almost complete within 40 min (Figure 2c). Because of the ultrafast polymerization kinetics, we did not observe the initial slow stage. However, the fast kinetics is consistent with the previously reported cooperative polymerization systems.[32,37] Monitoring changes in circular dichroism (CD) at 222 nm during the polymerization further confirmed the formation of right-handed α-helical structures (Figure S5). The initial slow increase in the CD signal at 222 nm in the first 90 s was

https://dx.doi.org/10.1021/jacs.0c01173
J. Am. Chem. Soc. 2020, 142, 8570−8574

consistent with the previously reported results, indicating two-stage cooperative polymerization kinetics.[32] In addition, compared with the typical slow polymerization initiated by hexylamine (monomer conversion of 37% within 24 h at the $[M]_0/[I]_0$ ratio of 100; Figure S6), such fast polymerization further indicated the cooperative NCA polymerization at the surface of the spherical macroinitiators.

To further confirm the necessity of α-helices to induce fast polymerization, we polymerized the racemic monomer (BDLG-NCA) instead of enantiopure monomers. It was observed that NCA monomers of $_L$ or $_D$ enantiomers can be polymerized at approximately the same rate (Figure 2d), and the PBDG polymer also showed predictable MWs and low dispersity values (Figure S7 and Table S3). However, racemic BDLG-NCA exhibited dramatically slower polymerization, and it took over 100 min to reach >98% monomer consumption at the $[M]_0/[I]_0$ ratio of 100, suggesting that the formation of α-helices was essential for the polymerization rate enhancement (Figures S8–S10). Additionally, the polymerization could not reach sufficient NCA consumption with racemic BDLG-NCA at higher DPs (>200), resulting in polymers with lower MWs than expected (Figure S11). GPC traces of the obtained racemic PBDLG polypeptide showed multiple distributions at higher DPs (>400), suggesting uncontrolled polymerization. These results thus collectively demonstrated that the well-controlled and rate-accelerating surface NCA polymerization was driven by interaction of neighboring α-helices.

As the interaction of α-helices can be affected by the surrounding environment, the effect of the solvent on the polymerization was then investigated. In another chlorinated solvent, chloroform ($CHCl_3$), the polymerization still featured excellent control, as exemplified by the high rate, accurate MWs, and low dispersities (Figure S12 and Table S4). However, when conducted in *N*,*N*-dimethylformamide (DMF), the polymerization was poorly controlled, yielding polymers with low MWs and extremely broad distributions (Figures S13 and S14). Increasing the $[M]_0/[I]_0$ ratio resulted in a negligible peak shift in the GPC traces, indicating the inability to get high-MW polypeptides. This occurred because DMF is a strongly polar solvent with a high dielectric constant, which could eliminate not only the hydrogen-bonding interactions between polypeptides and NCA monomers but also the electrostatic interactions resulting from the macrodipole moments of α-helices.[32,38] Taken together, these results confirmed that the surface NCA polymerization in nonpolar solvents can serve as a facile method to fabricate high-MW and monodisperse polypeptides.

It was expected that such low-dispersity polymers could form uniform spherical unimolecular micelles. In support of such an assumption, the sizes of the obtained polymers were determined by dynamic light scattering (DLS) after they were dissolved in DMF. Consist with their low dispersities, the polypeptides initiated by PAMAM initiators of different generations demonstrated extraordinarily narrow size distributions (Figures 3a,b and S15). In addition, the sizes of the unimolecular micelles were closely correlated to their MWs (Figure 3c), enabling precise control over the particle size by tuning the DP of the polymers. The sizes of the micelles were slightly bigger than the theoretical values at lower DPs (<400), which was largely attributed to the low initiation efficiency because of the ultrafast polymerization.[32] Cryogenic transmission electron microscopy (cryo-TEM) was further utilized to observe the morphology of the micelles. As expected, the

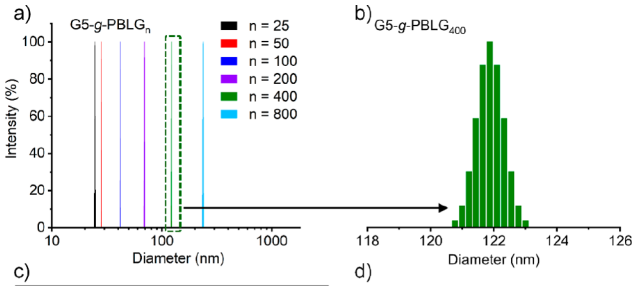

c)

Entry	Diameter (nm)	PDI
G5-*g*-PBLG$_{25}$	23.2 (12.9)*	0.097
G5-*g*-PBLG$_{50}$	28.4 (20.4)*	0.011
G5-*g*-PBLG$_{100}$	41.6 (35.4)*	0.021
G5-*g*-PBLG$_{200}$	71.5 (65.4)*	0.046
G5-*g*-PBLG$_{400}$	122.9 (125.4)*	0.073
G5-*g*-PBLG$_{800}$	238.0 (245.4)*	0.072

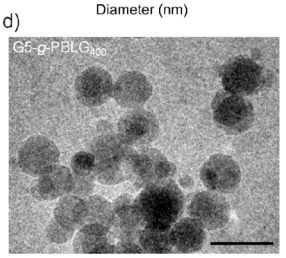

Figure 3. (a) Size distributions of various unimolecular micelles. (b) Amplified DLS histogram of G5-*g*-PBLG$_{400}$ micelles. (c) Diameters and dispersities of the unimolecular micelles determined by DLS (asterisks denote theoretical sizes). (d) Cryo-TEM image of G5-*g*-PBLG$_{400}$ micelles in DMF (scale bar = 200 nm).

micelles were spheroidal and uniform (Figure 3d). The contrast of the cryo-TEM image was not very clear because the solvent was DMF, not water. Because of the uniform structure, the initiation efficiency of the polymerization could be estimated assuming that the polymers grown from different surface amine groups had similar chain lengths. On the basis of the average length of an α-helix (0.15 nm per amino acid residue) and the size of G5 PAMAM (5.4 nm), the theoretical sizes of the unimolecular micelles can be obtained assuming an initiating efficiency of 100% (Figure 3C). Therefore, the initiation efficiencies of the G5-PBLG$_{50/100/200}$ polymers were estimated to be 65%, 83%, and 91%, respectively. The sizes of the micelles with higher DPs were nearly identical to the theoretical values, revealing that the initiation efficiencies were very close to 100%. After removal of the benzyl groups, uniform water-soluble poly($_L$-glutamic acid) unimolecular micelles were readily obtained (Figures S16–S20).

We next investigated whether the strategy can be utilized for other NCA monomers. First, we polymerized γ-(4-propargyloxybenzyl)-$_L$-glutamate *N*-carboxyanhydride (POBLG-NCA) in DCM. FT-IR study confirmed the fast conversion of POBLG-NCA (Figure S21), and GPC analysis showed that these polymers had accurate MW and narrow dispersity (Figure S22 and Table S5). DLS analysis demonstrated narrow size distributions of the unimolecular micelles (Figure S23). Additionally, other NCA monomers such as N^{ε}-benzyloxycarbonyl-$_L$-lysine *N*-carboxyanhydride (Lys(Z)-NCA) and γ-(4-allyloxylbenzyl)-$_L$-glutamate *N*-carboxyanhydride (AOBLG-NCA) can also be applied in the current system (Figures S24 and S25). These results suggested that size-controlled polypeptide-based unimolecular micelles bearing functional motifs can be readily fabricated.

In conclusion, we have reported an unprecedented NCA polymerization with high rates and superior polymerization control from the dendritic polymer surface. Polymers with extremely high MWs and low dispersities can be easily synthesized in the one-pot system. To the best of our knowledge, these are the highest-MW synthetic polypeptides reported to date. These polymers can form spherical

https://dx.doi.org/10.1021/jacs.0c01173
J. Am. Chem. Soc. 2020, 142, 8570–8574

unimolecular micelles with very narrow dispersities. This methodology enables precise control of the micelle size by tuning of the DP of the polymer, a feat seldom achieved in polymeric micellar systems. Monomers with reactive handles (e.g., alkynyl and alkenyl groups) can be utilized in this system, enabling the design of functional unimolecular micelles. Because of the intrinsic stability of the unimolecular micelles and the unique properties of polypeptides, this study provides a simple and robust strategy for the design of stable unimolecular polypeptide nanoparticles, which will find promising applications in the fields of biomimetic supramolecular chemistry, nanotechnology, and biomedicine.

■ ASSOCIATED CONTENT

Supporting Information

The Supporting Information is available free of charge at https://pubs.acs.org/doi/10.1021/jacs.0c01173.

Experimental procedures and characterizations (PDF)

■ AUTHOR INFORMATION

Corresponding Authors

Jianjun Cheng − *Department of Materials Science and Engineering, University of Illinois at Urbana−Champaign, Urbana, Illinois 61801, United States;* orcid.org/0000-0003-2561-9291; Email: jianjunc@illinois.edu

Lichen Yin − *Jiangsu Key Laboratory for Carbon-Based Functional Materials and Devices, Institute of Functional Nano and Soft Materials (FUNSOM), Collaborative Innovation Center of Suzhou Nano Science and Technology, Soochow University, Suzhou 215123, China;* orcid.org/0000-0002-4573-0555; Email: lcyin@suda.edu.cn

Authors

Shixian Lv − *Department of Materials Science and Engineering, University of Illinois at Urbana−Champaign, Urbana, Illinois 61801, United States; Jiangsu Key Laboratory for Carbon-Based Functional Materials and Devices, Institute of Functional Nano and Soft Materials (FUNSOM), Collaborative Innovation Center of Suzhou Nano Science and Technology, Soochow University, Suzhou 215123, China*

Hojun Kim − *Department of Materials Science and Engineering, University of Illinois at Urbana−Champaign, Urbana, Illinois 61801, United States; Center for Biomaterials, Biomedical Research Institute, Korea Institute of Science and Technology (KIST), Seoul 02792, Republic of Korea*

Ziyuan Song − *Department of Materials Science and Engineering, University of Illinois at Urbana−Champaign, Urbana, Illinois 61801, United States;* orcid.org/0000-0002-3165-3712

Lin Feng − *Department of Materials Science and Engineering, University of Illinois at Urbana−Champaign, Urbana, Illinois 61801, United States*

Yingfeng Yang − *Department of Materials Science and Engineering, University of Illinois at Urbana−Champaign, Urbana, Illinois 61801, United States*

Ryan Baumgartner − *Department of Materials Science and Engineering, University of Illinois at Urbana−Champaign, Urbana, Illinois 61801, United States*

Kuan-Ying Tseng − *Department of Materials Science and Engineering, University of Illinois at Urbana−Champaign, Urbana, Illinois 61801, United States*

Shen J. Dillon − *Department of Materials Science and Engineering, University of Illinois at Urbana−Champaign, Urbana, Illinois 61801, United States;* orcid.org/0000-0002-6192-4026

Cecilia Leal − *Department of Materials Science and Engineering, University of Illinois at Urbana−Champaign, Urbana, Illinois 61801, United States;* orcid.org/0000-0001-5972-508X

Complete contact information is available at: https://pubs.acs.org/10.1021/jacs.0c01173

Notes

The authors declare no competing financial interest.

■ ACKNOWLEDGMENTS

This research was financially supported by the U.S. National Science Foundation (CHE 1709820), the Ministry of Science and Technology of China (2016YFA0201200), the National Natural Science Foundation of China (51873142, 51573123, and 51722305), the 111 Project, and the Priority Academic Program Development of Jiangsu Higher Education Institutions (PAPD).

■ REFERENCES

(1) Amjad, M. W.; Kesharwani, P.; Mohd Amin, M. C. I.; Iyer, A. K. Recent advances in the design, development, and targeting mechanisms of polymeric micelles for delivery of siRNA in cancer therapy. *Prog. Polym. Sci.* **2017**, *64*, 154−181.

(2) Tang, Z.; He, C.; Tian, H.; Ding, J.; Hsiao, B. S.; Chu, B.; Chen, X. Polymeric nanostructured materials for biomedical applications. *Prog. Polym. Sci.* **2016**, *60*, 86−128.

(3) Su, L.; Li, R.; Khan, S.; Clanton, R.; Zhang, F.; Lin, Y.; Song, Y.; Wang, H.; Fan, J.; Hernandez, S.; Butters, A. S.; Akabani, G.; MacLoughlin, R.; Smolen, J.; Wooley, K. L. Chemical Design of Both a Glutathione-Sensitive Dimeric Drug Guest and a Glucose-Derived Nanocarrier Host to Achieve Enhanced Osteosarcoma Lung Metastatic Anticancer Selectivity. *J. Am. Chem. Soc.* **2018**, *140* (4), 1438−1446.

(4) Wang, D.; Lu, X.; Jia, F.; Tan, X.; Sun, X.; Cao, X.; Wai, F.; Zhang, C.; Zhang, K. Precision Tuning of DNA- and Poly(ethylene glycol)-Based Nanoparticles via Coassembly for Effective Antisense Gene Regulation. *Chem. Mater.* **2017**, *29* (23), 9882−9886.

(5) Deming, T. J. Synthesis of Side-Chain Modified Polypeptides. *Chem. Rev.* **2016**, *116* (3), 786−808.

(6) Lv, S.; Wu, Y.; Cai, K.; He, H.; Li, Y. J.; Lan, M.; Chen, X.; Cheng, J.; Yin, L. High Drug Loading and Sub-Quantitative Loading Efficiency of Polymeric Micelles Driven by Donor-Receptor Coordination Interactions. *J. Am. Chem. Soc.* **2018**, *140* (4), 1235−1238.

(7) Sun, X.; Wang, G.; Zhang, H.; Hu, S.; Liu, X.; Tang, J.; Shen, Y. The Blood Clearance Kinetics and Pathway of Polymeric Micelles in Cancer Drug Delivery. *ACS Nano* **2018**, *12* (6), 6179−6192.

(8) Eetezadi, S.; Ekdawi, S. N.; Allen, C. The challenges facing block copolymer micelles for cancer therapy: In vivo barriers and clinical translation. *Adv. Drug Delivery Rev.* **2015**, *91*, 7−22.

(9) Feiner-Gracia, N.; Buzhor, M.; Fuentes, E.; Pujals, S.; Amir, R. J.; Albertazzi, L. Micellar Stability in Biological Media Dictates Internalization in Living Cells. *J. Am. Chem. Soc.* **2017**, *139* (46), 16677−16687.

(10) Rosler, A.; Vandermeulen, G. W. M.; Klok, H. A. Advanced drug delivery devices via self-assembly of amphiphilic block copolymers. *Adv. Drug Delivery Rev.* **2012**, *64*, 270−279.

(11) Xu, H.; Yao, Q.; Cai, C.; Gou, J.; Zhang, Y.; Zhong, H.; Tang, X. Amphiphilic poly(amino acid) based micelles applied to drug delivery: The in vitro and in vivo challenges and the corresponding potential strategies. *J. Controlled Release* **2015**, *199*, 84−97.

(12) Wang, C.; Stayton, P. S.; Pun, S. H.; Convertine, A. J. Polymer nanostructures synthesized by controlled living polymerization for tumor-targeted drug delivery. *J. Controlled Release* **2015**, *219*, 345−354.
(13) Babin, J.; Leroy, C.; Lecommandoux, S.; Borsali, R.; Gnanou, Y.; Taton, D. Towards an easy access to amphiphilic rod-coil miktoarm star copolymers. *Chem. Commun.* **2005**, No. 15, 1993−1995.
(14) Zhou, Y.; Huang, W.; Liu, J.; Zhu, X.; Yan, D. Self-Assembly of Hyperbranched Polymers and Its Biomedical Applications. *Adv. Mater.* **2010**, *22* (41), 4567−4590.
(15) Hu, X.; Liu, G.; Li, Y.; Wang, X.; Liu, S. Cell-Penetrating Hyperbranched Polyprodrug Amphiphiles for Synergistic Reductive Milieu-Triggered Drug Release and Enhanced Magnetic Resonance Signals. *J. Am. Chem. Soc.* **2015**, *137* (1), 362−368.
(16) Rhodes, A. J.; Deming, T. J. Tandem Catalysis for the Preparation of Cylindrical Polypeptide Brushes. *J. Am. Chem. Soc.* **2012**, *134* (47), 19463−19467.
(17) Wang, D.; Zhao, T.; Zhu, X.; Yan, D.; Wang, W. X. Bioapplications of hyperbranched polymers. *Chem. Soc. Rev.* **2015**, *44* (12), 4023−4071.
(18) Mullner, M.; Dodds, S. J.; Nguyen, T. H.; Senyschyn, D.; Porter, C. J. H.; Boyd, B. J.; Caruso, F. Size and Rigidity of Cylindrical Polymer Brushes Dictate Long Circulating Properties In Vivo. *ACS Nano* **2015**, *9* (2), 1294−1304.
(19) Li, Z.; Ma, J.; Lee, N. S.; Wooley, K. L. Dynamic Cylindrical Assembly of Triblock Copolymers by a Hierarchical Process of Covalent and Supramolecular Interactions. *J. Am. Chem. Soc.* **2011**, *133* (5), 1228−1231.
(20) Fan, X.; Li, Z.; Loh, X. J. Recent development of unimolecular micelles as functional materials and applications. *Polym. Chem.* **2016**, *7* (38), 5898−5919.
(21) Rzayev, J. Molecular Bottlebrushes: New Opportunities in Nanomaterials Fabrication. *ACS Macro Lett.* **2012**, *1* (9), 1146−1149.
(22) Sun, G.; Cho, S. H.; Clark, C.; Verkhoturov, S. V.; Eller, M. J.; Li, A.; Pavia-Jimenez, A.; Schweikert, E. A.; Thackeray, J. W.; Trefonas, P.; Wooley, K. L. Nanoscopic Cylindrical Dual Concentric and Lengthwise Block Brush Terpolymers as Covalent Preassembled High-Resolution and High-Sensitivity Negative-Tone Photoresist Materials. *J. Am. Chem. Soc.* **2013**, *135* (11), 4203−4206.
(23) Dang, J.; Ye, H.; Li, Y.; Liang, Q.; Li, X.; Yin, L. Multivalency-assisted membrane-penetrating siRNA delivery sensitizes photothermal ablation via inhibition of tumor glycolysis metabolism. *Biomaterials* **2019**, *223*, 119463.
(24) Sheiko, S. S.; Sumerlin, B. S.; Matyjaszewski, K. Cylindrical molecular brushes: Synthesis, characterization, and properties. *Prog. Polym. Sci.* **2008**, *33* (7), 759−785.
(25) Thota, B. N. S.; Urner, L. H.; Haag, R. Supramolecular Architectures of Dendritic Amphiphiles in Water. *Chem. Rev.* **2016**, *116* (4), 2079−2102.
(26) Byrne, M.; Murphy, R.; Kapetanakis, A.; Ramsey, J.; Cryan, S. A.; Heise, A. Star-Shaped Polypeptides: Synthesis and Opportunities for Delivery of Therapeutics. *Macromol. Rapid Commun.* **2015**, *36* (21), 1862−1876.
(27) Byrne, M.; Mildner, R.; Menzel, H.; Heise, A. Glycosylated Star Polypeptides from NCA Polymerization: Selective Binding as a Function of Degree of Branching and Glycosylation. *Macromol. Biosci.* **2015**, *15* (1), 74−81.
(28) Fan, J.; Borguet, Y. P.; Su, L.; Nguyen, T. P.; Wang, H.; He, X.; Zou, J.; Wooley, K. L. Two-Dimensional Controlled Syntheses of Polypeptide Molecular Brushes via N-Carboxyanhydride Ring-Opening Polymerization and Ring-Opening Metathesis Polymerization. *ACS Macro Lett.* **2017**, *6* (9), 1031−1035.
(29) Dalsin, S. J.; Hillmyer, M. A.; Bates, F. S. Linear Rheology of Polyolefin-Based Bottlebrush Polymers. *Macromolecules* **2015**, *48* (13), 4680−4691.
(30) Mai, Y.; Xiao, L.; Eisenberg, A. Morphological Control in Aggregates of Amphiphilic Cylindrical Metal-Polymer "Brushes. *Macromolecules* **2013**, *46* (8), 3183−3189.
(31) Hortz, C.; Birke, A.; Kaps, L.; Decker, S.; Wachtersbach, E.; Fischer, K.; Schuppan, D.; Barz, M.; Schmidt, M. Cylindrical Brush Polymers with Polysarcosine Side Chains: A Novel Biocompatible Carrier for Biomedical Applications. *Macromolecules* **2015**, *48* (7), 2074−2086.
(32) Baumgartner, R.; Fu, H. L.; Song, Z.; Lin, Y.; Cheng, J. Cooperative polymerization of alpha-helices induced by macromolecular architecture. *Nat. Chem.* **2017**, *9* (7), 614−622.
(33) Chen, C.; Fu, H.; Baumgartner, R.; Song, Z.; Lin, Y.; Cheng, J. Proximity-Induced Cooperative Polymerization in "Hinged" Helical Polypeptides. *J. Am. Chem. Soc.* **2019**, *141* (22), 8680−8683.
(34) Ren, Y.; Baumgartner, R.; Fu, H. L.; van der Schoot, P.; Cheng, J. J.; Lin, Y. Revisiting the Helical Cooperativity of Synthetic Polypeptides in Solution. *Biomacromolecules* **2017**, *18* (8), 2324−2332.
(35) Lu, H.; Cheng, J. *N*-Trimethylsilyl Amines for Controlled Ring-Opening Polymerization of Amino Acid *N*-Carboxyanhydrides and Facile End Group Functionalization of Polypeptides. *J. Am. Chem. Soc.* **2008**, *130* (38), 12562−12563.
(36) Soteriou, A.; Gamage, M.; Trinick, J. A Survey of Interactions Made by the Giant Protein Titin. *J. Cell Sci.* **1993**, *104*, 119−123.
(37) Song, Z.; Fu, H.; Wang, J.; Hui, J. S.; Xue, T.; Pacheco, L. A.; Yan, H.; Baumgartner, R.; Wang, Z.; Xia, Y.; Wang, X.; Yin, L.; Chen, C.; Rodriguez-Lopez, J.; Ferguson, A. L.; Lin, Y.; Cheng, J. Synthesis of polypeptides via bioinspired polymerization of in situ purified N-carboxyanhydrides. *Proc. Natl. Acad. Sci. U. S. A.* **2019**, *116* (22), 10658−10663.
(38) Song, Z.; Fu, H.; Baumgartner, R.; Zhu, L.; Shih, K.-C.; Xia, Y.; Zheng, X.; Yin, L.; Chipot, C.; Lin, Y.; Cheng, J. Enzyme-mimetic self-catalyzed polymerization of polypeptide helices. *Nat. Commun.* **2019**, *10*, 5470.

https://dx.doi.org/10.1021/jacs.0c01173
J. Am. Chem. Soc. 2020, 142, 8570−8574